J. Synchrotron Rad. (1998). **5**, 687–689

Focusing and reflection by a bent crystal for high-energy synchrotron radiation

Hitoshi Yamaoka,* Kiyotaka Ohtomo† and Tetsuya Ishikawa

The Institute of Physical and Chemical Research (RIKEN), Mikazuki, Sayo, Hyogo 679-5143, Japan.
E-mail: yamaoka@spring8.or.jp

(*Received 4 August 1997; accepted 2 December 1997*)

The focusing properties and resolution of a doubly bent crystal in the Bragg case have been analytically studied from a geometrical viewpoint. Simulation using the Takagi–Taupin equations was also performed for singly bent crystal reflections to study the reflectivity. The critical radius of curvature for changing from dynamical to kinematical diffraction is calculated to be of the order of a few tens of metres for an Si 400 reflection of 110 keV X-rays.

Keywords: monochromators; doubly bent; dynamical; kinematical; high-energy synchrotron radiation.

1. Introduction

The resolution of a bent-crystal monochromator is determined by the natural width of the crystal, the crystal perfection, the deviation of the crystal curvature from the ideal one, and the distortion due to heat load or other reasons. When a crystal is bent to focus the beam, not only the energy spread but also the integrated intensity normally changes. Depending on the experiments, there should be an optimum bending radius and focusing condition. In the SPring-8 beamline BL08W, two kinds of single-crystal monochromators are installed. Both types are bent for inelastic scattering experiments (Sakurai *et al.*, 1995). One is a doubly bent crystal to reflect 100–150 keV photons and the other is a singly bent crystal for 300 keV photons (Yamaoka *et al.*, 1996, 1998). Here we present a simple analysis for a doubly bent crystal to determine geometrically the optimum focusing condition for high-energy synchrotron radiation. At high energies, greater than ~100 keV, when a crystal is bent the reflection changes gradually from dynamical to kinematical as a function of the radius of curvature. A simple calculation is performed by using an analytical formula for a lamellar model. We also simulate a bent crystal for 110 keV photons using Takagi–Taupin equations to confirm our analytical analysis. In these calculations the crystal is singly bent for simplicity.

2. Focusing of a doubly bent crystal

Two coordinate systems, (x, y, z) and (X, Y, Z), are introduced, as shown in Fig. 1(*a*). The wavevector of incident X-rays, $\mathbf{k}$, is expressed in (x, y, z) coordinates as $\mathbf{k} = k(\cos\sigma_z \sin\sigma_x, \cos\sigma_z \cos\sigma_x, \sin\sigma_z)$. The reciprocal lattice vector, $\mathbf{h}$, is written in (X, Y, Z) coordinates as $\mathbf{h} = (-h_X, -h_Y, h_Z)$. Taking $\tan\xi = -h_X/h_Z$, $\tan\eta = -h_Y/h_Z$ and $h^2 = h_X^2 + h_Y^2 + h_Z^2 = h_Z^2(\tan^2\xi + \tan^2\eta + 1)$, we may write

$$\mathbf{h} = h/(\tan^2\eta + \tan^2\xi + 1)^{1/2}(-\tan\xi, -\tan\eta, 1), \qquad (1)$$

where $h = |\mathbf{h}|$. The coordinate systems are related by

$$\begin{pmatrix} x \\ y \\ z \end{pmatrix} = \begin{pmatrix} 1 & 0 & 0 \\ 0 & \cos\theta & -\sin\theta \\ 0 & \sin\theta & \cos\theta \end{pmatrix} \begin{pmatrix} X \\ Y \\ Z \end{pmatrix},$$

where θ is the incident angle of the X-rays. The reciprocal lattice vector in (x, y, z) coordinates is

$$\mathbf{h} = h/(\tan^2\xi + \tan^2\eta + 1)^{1/2} \times \big(-\tan\xi, -\tan\eta\cos\theta - \sin\theta, -\tan\eta\sin\theta + \cos\theta\big). \qquad (2)$$

From the Bragg relation, $\mathbf{k}_h = \mathbf{k} + \mathbf{h}$ and $|\mathbf{k}| = |\mathbf{k}_h|$, the angle deviation, $\delta\theta$, from the Bragg angle of a doubly bent crystal at point A in Fig. 1 is written as

$$\delta\theta = \theta_{\rm inc} - \theta_{\rm B} = \arcsin(-\mathbf{k}.\mathbf{h}/kh) - \theta_{\rm B} \qquad (3)$$

$$= \arcsin\Big\{-1/(\tan^2\eta + \tan^2\xi + 1)^{1/2} \times \big[-\tan\xi\cos\sigma_z\sin\sigma_x - \cos\sigma_z\cos\sigma_x(\tan\eta\cos\theta + \sin\theta) + \sin\sigma_z(-\tan\eta\sin\theta + \cos\theta)\big]\Big\} - \theta_{\rm B}. \qquad (4)$$

When $\theta_{\rm inc} = \theta_{\rm B}$, (4) is written approximately as

$$2\xi\sigma_x - 2\eta\cos\theta - (\xi^2 + \sigma_x^2 + \eta^2)\sin\theta \simeq 0. \qquad (5)$$

Normally we can derive the angles of ξ and η from the approximate relation $\xi \simeq p\sigma_x/N$ and $\eta \simeq p\sigma_z/(R\sin\theta)$, where p, N and R are the distance from source to crystal, sagittal radius and meridian radius, respectively. In (4), if we set $\sigma_x = 0$, $\xi = 0$ and $\theta = \theta_{\rm B}$, the angle deviation becomes $\delta\theta = \eta - \sigma_z$. When $\delta\theta = 0$, $\eta = \sigma_z$. Then we can obtain the relation $p = R\sin\theta$ and $q/p = 1$ for symmetrical reflections, where q is the distance from the crystal to the focus point. If $\eta = \sigma_z$, $\theta = \theta_{\rm B}$ and $\delta\theta = 0$ in (4), the following relation is approximately derived neglecting higher-

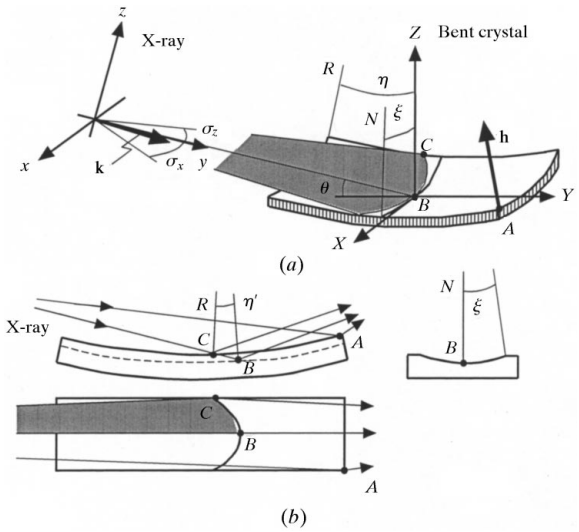

Figure 1
(*a*) Coordinate system. $\mathbf{k}$, $\mathbf{h}$, R and N are the wavevector of the incident beam, the reciprocal lattice vector of the crystal, the meridional radius and the sagittal radius, respectively. (*b*) Another point C on the crystal surface that affects the angle deviation.

† On leave from Quantum Equipment Division, Sumitomo Heavy Industrial Ltd, Japan.

order terms, $2\xi\sigma_x - (\xi^2 + \sigma_x^2)\sin\theta \simeq 0$. Then we find

$$N = (1 - \cos\theta)p/\sin\theta. \quad (6)$$

It is noted that at small incident angles the above result agrees with the relation $N' = p\sin\theta/2$ derived from the known relation $N' = 2pq\sin\theta/(p+q)$ when $q/p = 1/3$. In practice, the ratio $(N - N')/N$ is less than 1% for incident angle less than 10°. Figs. 2(*a*) and 2(*b*) show examples of the energy spread of the Si 400 reflection as a function of the ratio q/p (magnification), and incident energy from 100 keV to 150 keV where p = 41.2 m, σ_z = 0.06 mrad and σ_x = 0.4 mrad. In Fig. 2(*a*), the sagittal bend radius, N (or the magnification), is varied while the meridional bend radius, R, is constrained to satisfy the optimum condition $q/p = 1$. In Fig. 2(*b*), conversely, R (or the magnification) is varied while N is constrained to satisfy the optimum condition expressed in (6). To understand the results easily, we use the magnification (q/p) as a parameter in Fig. 2 and in the calculation the value of the magnification is substituted into (6) for sagittal focus and $R = 2pq/(p+q)/\sin\theta$ for meridian focus, respectively. The optimum focus point of the sagittal focus that minimizes the energy spread is apparently different from that of the meridian focus. To coincide the two (meridian and sagittal) focus points, we can utilize a crystal cut asymmetrically in the meridional direction.

Another possible angle deviation is caused by the reflection at point C in Fig. 1(*b*) (Kawata *et al.*, 1998). We take into account the depth effect along the Z direction in Fig. 1 for the incident X-rays of $\sigma_z = 0$ that land at the location with different η and different Z. In Fig. 1(*b*), η' is written as $\eta' = N(1 - \cos\xi)/(R\tan\theta)$. Figs. 2(*c*) and 2(*d*) show the results when η' is substituted into (4) instead of η under the condition of $\sigma_z = 0$ for sagittal focus and meridional focus, respectively. For changing N there is an optimum for the magnification at about 0.2. For changing R the deviation monotonously decreases as a function of the magnification, as shown in Fig. 2(*d*). It is noted that if we choose the focusing condition so that q/p = 1/3 in the sagittal direction and q/p = 1 in the meridian direction, the angle deviation at the point C gives a wider energy spread than that at point B. This fact will be more important when high resolution is required in the experiment.

It is worthwhile to make an additional remark about a double-crystal arrangement. Koyama *et al.* (1992) showed the effect of misalignment in a double-crystal reflection with sagittal focus. If there was no misalignment, the relation $N' = p\sin\theta/2$ was derived for the sagittal focus. This indicates that N' gives minimum angle deviation at any incident angle in the double-crystal case, while, in the corresponding relation for the single-crystal case, given by N in (6), N is almost the same as N' at low incident angles, as shown above.

3. Reflection of a singly bent crystal

The integrated reflectivity and the width of the reflectivity curve have been calculated in the Bragg case using a simple formula derived for a lamellar model, as shown in Fig. 3 (Erola *et al.*, 1990). The following conditions were chosen for the two calculations: Si 400 symmetric reflection at 110 keV, and Si 771 reflection with asymmetry angle of 1° at 300 keV, respectively. There are critical radii for the integrated reflectivities: ~50 m for the 110 keV reflection and $\sim 10^4$ m for the 300 keV reflection. In practice, the bending radius of the 100–150 keV monochromator crystal in the SPring-8 BL08W is much higher than the above value. For a 100–150 keV monochromator, dynamical diffraction still dominates. For a 300 keV monochromator, where the radius is much less than the above critical radius, kinematical diffraction is expected.

The effects on the angle resolution when the crystal is bent have been studied by simulations using the Takagi–Taupin equations. The simulation code *ODDS* (*Optics for Distorted*

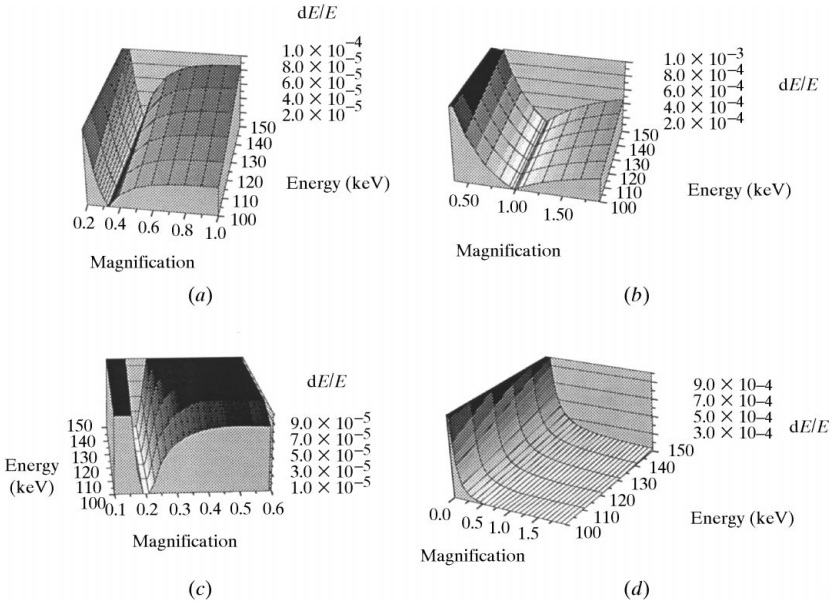

Figure 2
(*a*) Sagittal focusing as a function of incident energy from 100 to 150 keV and the magnification at point A when $\sigma_z = \eta$ is assumed and η is used. dE/E is the energy spread and the magnification corresponds to q/p. The following parameters are used: Si 400 reflection; p = 41.2 m; σ_z = 0.06 mrad and σ_x = 0.4 mrad. (*b*) Meridional focusing as a function of incident energy and the magnification at point A when equation (6) is assumed and η is used. (*c*) Sagittal focusing as a function of incident energy and the magnification at point C when $\sigma_z = \eta$ is assumed and η' is used. (*d*) Meridional focusing as a function of incident energy and the magnification at point C when equation (6) is assumed and η' is used.

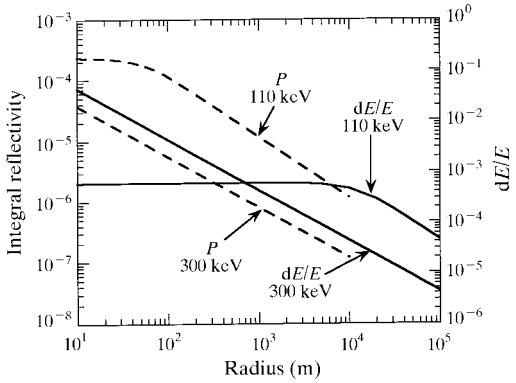

Figure 3
Calculated results of integrated reflectivity and energy spread by an analytical formula for a lamellar model as a function of radius of curvature of a singly bent crystal in the Bragg case.

Crystal of Diffraction Simulation; Ohtomo & Ishikawa, 1995) was used. Fig. 4(*a*) shows the reflectivity curves of the Si 400 symmetrical reflection at 110 keV (Bragg angle of 2.379° and Σ polarization) for several bending radii of curvature. W is the normalized angle deviation from the Bragg condition (the same as y in the text by Zachariasen, 1945). Here the deformation, u, of the crystal is included in the simulation according to

$$u_x = [R + (t/2) - y]\sin[x/(R + t/2)], \quad (7)$$

$$u_y = [R + (t/2) - y]\{1 - \cos[x/(R + t/2)]\}, \quad (8)$$

where R, t and (x, y) are the radius of curvature, crystal thickness and original crystal position, respectively. The calculations were performed to a depth of 100 μm, much greater than the extinction distance, with a mesh of 1000 points in depth and 4985 points in a length of 24 mm. Fig. 4(*b*) shows the integrated intensity and the energy spread in Fig. 4(*a*) as a function of radius of curvature. Fig. 4 shows that the critical radius is ∼20 m, so the order of the magnitude of the critical radius agrees with that in Fig. 3. From these results it is concluded that at ∼100 keV the dynamical effect is dominant for a bending radius of the order of a few tens of metres, whereas at ∼300 keV the kinematical effect dominates for almost any bent crystal. This means that when a crystal is bent to have a radius of the order of a few hundred metres, as used at SPring-8, an increase in the integral intensity for the reflected beam would not be expected at around 100 keV. Mosaic crystals are one of the candidates for obtaining a much higher integral intensity for a 100 keV photon beam reflection (Yamaoka *et al.*, 1997).

We thank Professor H. Kawata and Mr M. Sato of KEK for useful discussions about the resolution of a bent crystal. HY is grateful to Dr Y. Sakurai of RIKEN and Professor N. Sakai of HIT for their encouragement.

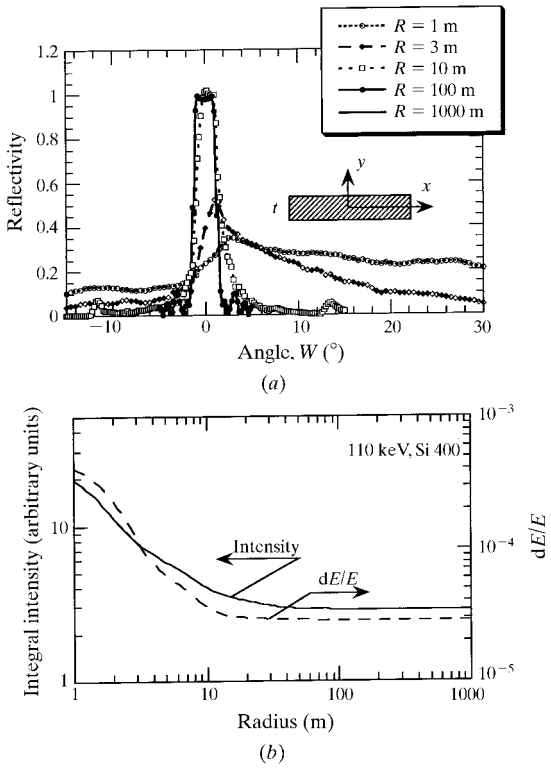

Figure 4
(*a*) Simulation results using the Takagi–Taupin equations for various radii of curvature for the Si 400 reflection at 110 keV with the (x, y) coordinate system used in the calculation, where t is the crystal thickness. A beam width of 1 mm, constant intensity profile and Σ polarization are assumed. (*b*) Integrated intensity of the reflectivity curves as a function of bending radius derived from the results of (*a*).

References

Erola, E., Eteläniemi, V., Suortti, P., Pattison, P. & Thomlinson, W. (1990). *J. Appl. Cryst.* **23**, 35–42.
Kawata, H., Sato, M., Higashi, Y. & Yamaoka, H. (1998). *J. Synchrotron Rad.* **5**, 673–675.
Koyama, A., Nomura, M., Kawata, H., Iwazumi, T., Sato, M. & Matsushita, T. (1992). *Rev. Sci. Instrum.* **63**, 916–919.
Ohtomo, K. & Ishikawa, T. (1995). *SPring-8 Annual Report 1994*, pp. 212–213. JASRI, Mikazuki, Sayo, Hyogo 679-5198, Japan.
Sakurai, Y., Yamaoka, H., Kimura, H., Marechal, X. M., Ohtomo, K., Mochizuki, T., Ishikawa, T., Kitamura, H., Kashiwara, Y., Harami, T., Tanaka, Y., Kawata, H., Shiotani, N. & Sakai, N. (1995). *Rev. Sci. Instrum.* **66**, 1774–1776.
Yamaoka, H., Goto, S., Kohmura, Y., Uruga, T. & Ito, M. (1997). *Jpn. J. Appl. Phys.* **36**, 2792–2799.
Yamaoka, H., Mochizuki, T., Sakurai, Y. & Kawata, H. (1998). *J. Synchrotron Rad.* **5**, 699–701.
Yamaoka, H., Sakurai, Y., Mochizuki, T., Ohtomo, K. & Kawata, H. (1996). *SPring-8 Annual Report 1995*, pp. 195–196. JASRI, Mikazuki, Sayo, Hyogo 679-5198, Japan.
Zachariasen, W. H. (1945). *Theory of X-ray Diffraction in Crystals.* New York: John Wiley.